

Detecting and localizing the foci in human epileptic seizures

Eshel Ben-Jacob¹, Stefano Boccaletti^{2,3}, Anna Pomyalov³, Itamar Procaccia³ and Vernon L. Towle⁴

¹ School of Physics and Astronomy, Tel Aviv University, Tel Aviv 69978, Israel

² Embassy of Italy in Tel Aviv, Trade Tower, 25 Hamered St., Tel Aviv 68125, Israel

³ Department of Chemical Physics, The Weizmann Institute of Science, Rehovot 76100, Israel

⁴ Dept. of Neurology, The University of Chicago, 5841 S. Maryland Ave., Chicago, IL 60637

(Dated: February 9, 2020)

We consider the electrical signals recorded from a subdural ECoG grid of electrodes placed on the pial surface of the brain for chronic evaluation of epileptic patients before surgical resection. A simple and computationally fast method to analyze the inter-ictal phase synchrony between such electrodes is introduced and developed with the aim of detecting and localizing the foci of the epileptic events. We evaluate the method by comparing the results of surgery to the localization predicted here. We find an indication of good correspondence between the success or failure in the surgery and the agreement between our identification and the regions actually operated on.

Epilepsy is defined as recurrent seizures due to an excessive discharge of cerebral neurons, as a result of disturbances in normal functioning, and associated with a variety of clinical and laboratory manifestations. Epilepsy is one of the today's most common neurological disorder, with more than 50 million people affected worldwide.

Those patients who do not respond satisfactorily to medications are surgical candidates.

Localizing accurately the epileptic focus (or foci) is therefore an essential first stage for surgeons, who need to make sure that they are going after the real source of the seizure, thus minimizing the surgery's invasiveness.

I. INTRODUCTION

Epilepsy is defined as an unprovoked seizure due to an excessive discharge of cerebral neurons, occurring as a result of disturbances in normal functioning, and associated with a variety of clinical and laboratory manifestations. Today, epilepsy is the world's most common neurological disorder, with more than 50 million people affected worldwide.

Roughly 30-40% of patients do not respond satisfactorily to medications, and about 20% are surgical candidates [1]. This is specially true for focal epilepsy. During the focal seizures the electric signals from one particular group (or some localized groups) of neurons (the focus) occasionally become so strong that they overwhelm the signals of neighboring cells. These signals can quickly spread from one side of the brain to the other, determining several symptoms: blank stare, out-of-control tremors, loss of motor control, and violent convulsions.

As a part of presurgical evaluation electrodes are placed directly on the surface of the brain to find the seizure's source. The grids, consisting of 50 to 100 electrodes spatially distributed over the suspected focal region are placed on the pial surface of the brain (see Figure 1), and the ensemble of signals [called the electrocorticogram (ECoG)] is simultaneously recorded and an-

alyzed for detecting the proper brain area to be resected [2]. Each electrode detects the local field potential of a small brain area [3]. Decisions regarding which brain areas to resect are based in part on a visual inspection of the ECoG signals by a board certified team of physicians who identify the electrodes showing signal patterns similar to those appearing during the epileptic seizure.

The clinical challenge is how to analyze the ECoG signals to achieve a simple, automatic, data-driven, fast and reliable identification of the epileptic focus. Traditionally, linear measures, such as correlation coefficients, were utilized for the complementary data analysis. In the last two decades methods based on the non-linear measures were introduced to the field.

It has been shown that a significant reduction of the dimension of the system [4, 5] (as measured by the correlation dimension [6] and by the neuronal complexity loss) occur in the vicinity of the epileptic focus, not only during the seizure (so-called ictal periods), but also between the seizures (the inter-ictal periods).

The interdependence between signals from different sites, studied by means of nonlinear cross-predictability and mutual non-linear predictability [7, 8], also allows the location of the focus. Surrogate-corrected non-linear measures [9] were shown to correctly identify the focal hemisphere in the inter-ictal recordings. Many of these methods involve the reconstruction of the phase space by time-delay embedding [10]. The latter requires knowledge of the autocorrelation time (which for this type of signals may vary by an order of magnitude within a short time) and a number of time points that scales as 10^D , where D is the dimension of the phase-space attractor [11]. But, on the other hand, the non-stationary nature of EEG signals requires analysis over relatively short time windows with number of time-points of the order of 10^3 . Therefore, one should exercise extreme caution when drawing conclusions from the analysis involving high dimensional embedding. Even if all precautions are taken, such calculations are computationally costly.

Recently, concepts from synchronization analysis were brought to the study of ECoG signals [12, 13, 14, 15, 16, 17], leading to a series of promising results on localization

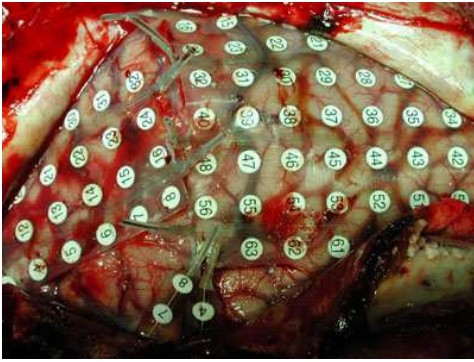


FIG. 1: (Color online) Subdural ECoG grid of electrodes placed on the pial surface of the brain for chronic evaluation of epileptic patients before surgical resection.

and predictability of epileptic seizures. In most of these works the increase in the synchronization was found only during the seizure, while synchronization clusters identified in [15], remain synchronized also during inter-ictal periods. Similar stability of local hyper-synchronous regions was found also in [16]. In spite of demonstrated success, formulation of these methods involve a number of assumptions, that we would like to relax in our proposed approach.

The aim of this paper is twofold. First, we describe a model-free and fast approach, based on phase synchronization, that is able to identify the epileptic focus. Second, we apply the method to ECoG data of three patients, and show that there is a good correspondence between the success or failure in surgery and the the overlap between the area spanned by the electrodes identified by our method and that of the brain tissue actually removed.

II. METHOD

To see the main concepts behind the method, consider a one-dimensional oscillatory signal $x(t)$. The associated phase space can be fully reconstructed by using the coordinates $x(t)$, $dx(t)/dt$, $d^2x(t)/dt^2$; ..., with as many derivatives as needed to exhaust the dimensionality of the system. In such a reconstructed phase space one can then define the Poincare section by noting the points obtained when the orbit crosses the surface $dx(t)/dt = 0$. Obviously, this surface coincides with the points of minimum or maximum in the original one-dimensional signal $x(t)$. In this work we focus on the points of maximum, and define the phase $\phi(t)$ of the trajectory by increasing its value by 2π after each maximum. Precisely, in between the k th maximum occurring at $t = t_k$ and the $(k+1)$ th maximum occurring at t_{k+1} , we define the phase for all time $t_k < t < t_{k+1}$ using the linear interpolation [18]

$$\phi(t) = 2\pi k + 2\pi \frac{t - t_k}{t_{k+1} - t_k} \quad (t_k < t < t_{k+1}) : \quad (1)$$

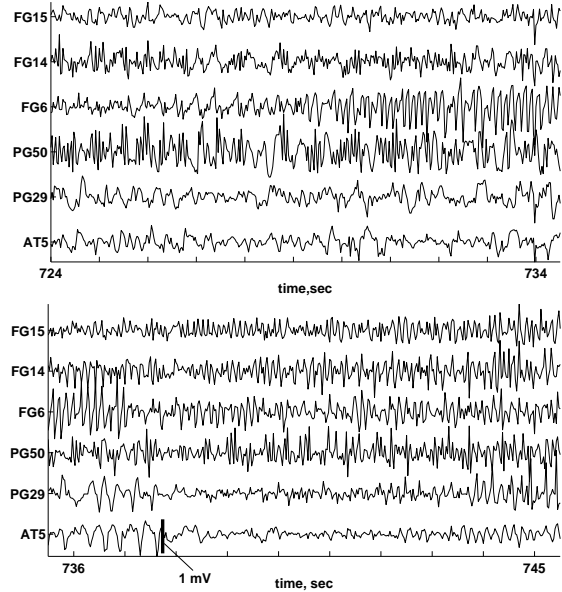


FIG. 2: Voltage traces of ECoG signals. Two 10 s portions of voltage traces of 6 electrodes, taken from a multielectrode recording of 96 electrodes of patient B, cf. Fig. 10. The analysis below indicates that the signals coming from electrodes FG 6, FG 14, FG 15 and PG 50 belong to the epileptic foci, whereas the PG 29 and AT 5 do not. The voltage scale of 1 mV is shown at the last AT 5 line.

Note that the resulting monotonically increasing phase does not contain any information about the amplitude of the original signal and the results of the analysis are not affected by the amplitude variation [19].

Phases can be affected by instrumental artifacts; we have carefully ascertained that any signal segments that appear identical in all recording channels were excluded from the signal prior to calculation of the phases. It is important to remark that our data feature broad band spectra. Alternative measures of the phase (such as the one based on the Hilbert transform) imply the presence of a prominent spectral peak [18]. We would like to avoid any a priori assumptions on the spectral structure of the signals, therefore we opted for the above definition of phase, Eq. 1.

The notion of phase synchronization [18] refers to a process wherein a locking of the phases of weakly coupled oscillators is produced, without implying a substantial correlation in the oscillators' amplitudes. The same concept can be related to our case, for measuring the degree of phase synchronization of two different signals, say $x(t)$ and $y(t)$. Using the basic definition (1), one can indeed produce the phases of each signal, denoted as $\phi_x(t)$ and $\phi_y(t)$, respectively. Taking $x(t)$ as the reference signal, one can further consider the time points of its maximum t_k , and read the phase $\phi_y(t_k)$ at these time points. One then defines the following reduced phases

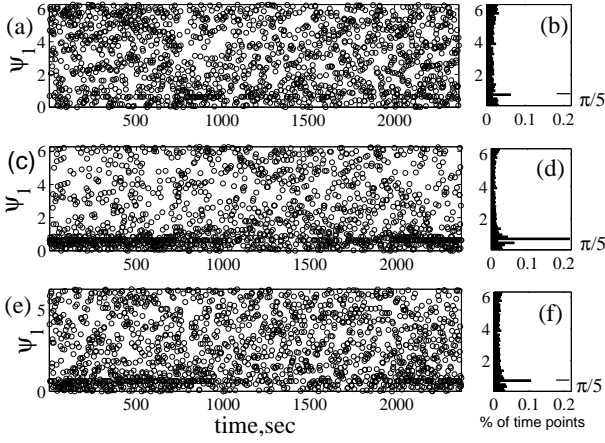


FIG. 3: Panels (a), (c) and (e): Synchrograms for 3 neighboring pairs of electrodes along [FG 13-FG 14 (a), FG 15-FG 14 (c)] and across the grid [FG 6-FG 14 (e)], calculated for the reference electrode FG 14 (the signals for FG 6, FG 14 and FG 15 are shown in Fig 2). Since the synchronization line appears at $\psi_1 = 0$, a small all phase offset of $\pi/5$ was added to the phase ψ_1 for clarity. Panels (b), (d), and (f) show the histograms of the time points distribution within the corresponding synchrogram. Clearly, only one strong line is present in each synchrogram, at the position of the offset phase ($\pi/5$). This corresponds to the 1:1 synchronization without visible phase difference.

$\psi_m(t_k)$ according to

$$\begin{aligned} \psi_1(t_k) &= \psi(t_k) \bmod 2\pi; \\ \psi_2(t_k) &= \psi(t_k) \bmod 4\pi; \\ &\vdots; \\ \psi_m(t_k) &= \psi(t_k) \bmod 2m\pi. \end{aligned} \quad (2)$$

The graphic representation of $\psi_m(t_k)$ vs. t_k is called a synchrogram of order m . We will consider the signals $x(t)$ and $y(t)$ as synchronized at ratio $n:m$ when the m th order synchrogram exhibits n distinct horizontal lines (i.e. reduced phase $\psi_m(t_k)$ for a series of time t_k). Synchrograms, indeed, have been proved to be useful to visualize and trace transitions between different ratios of phase locking in biological data, as the cardiorespiratory system of a human subject [20], where non-stationarity is often strong. Note that $\psi_m(t_k)$ is, in general, not symmetric and within the same pair of signals may depend on which electrode is taken as a reference.

To exemplify this notion in the present context, we present in Fig. 3 synchrograms constructed from the signals associated with three neighboring pairs of electrodes, which display the presence of 1:1 phase synchronization. The fraction of the time, during which the signals are synchronized, differs significantly, albeit the same geometrical distance.

To test for the presence of more complicated synchronization ratios, we calculated the synchrograms of higher orders. The histograms for them are shown in Fig 4. The number of strong lines in each histogram is equal to the

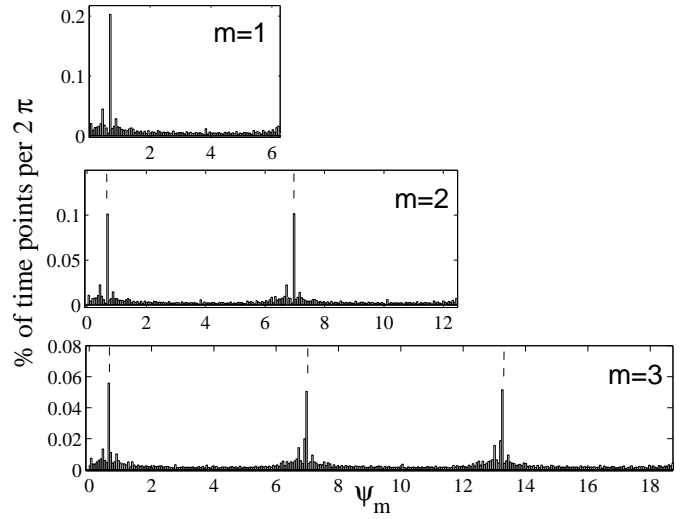


FIG. 4: Histograms for synchrograms of orders $m = 1; 2$ and 3 calculated for the pair of electrodes FG 14-FG 15 (cf. Fig 3, c and d). The dashed lines mark offset positions $\pi/5; 2\pi/5$ and $4\pi/5$. The same bins size ($\Delta\psi = 100$) was used in all histograms. The number of strong lines equals to the order of the synchrogram, confirming the 1:1 synchronization. The position of the synchronization lines coincide with the value of the offset phase within one bin.

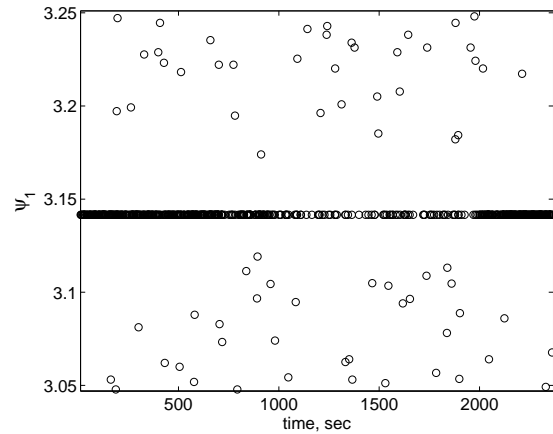


FIG. 5: The vicinity of the 1:1 synchronization line for synchrogram of electrodes FG 14 and FG 15, with the phase offset $\pi/5$. Note that the synchronization line is clearly isolated.

order of the corresponding synchrogram, thus confirming the dominant 1:1 synchronization ratio. Note, that this ratio is usually assumed in the methods involving phase difference [5, 15, 16]. We do not make such an assumption. In fact, any synchronization ratio may be treated on the same footing. The analysis of long (several hours) recordings reveal occasional appearance of additional ratios of synchronization (1:2 and higher, always repeated as a group in higher order synchrograms), although they are weaker and do not affect the strength on the main 1:1 synchronization ratio. In the following analysis we concentrate on the first order synchrograms ψ_1 with the

phase offset equal to π . The phase points that belong to the synchronization line may be easily extracted from the synchrogram, since they are clearly isolated from other points (see Fig 5).

The present method shares some similarities with the so-called event-synchronization technique [13], though this latter strategy is, in general, unable to distinguish between different types of nonlinear lockings.

III. RESULTS AND DISCUSSION

A. Patients and ECoG recordings

In this paper we analyze the ECoG data of three female patients with intractable partial complex seizures with secondary generalization, referred to as patients A, B and C, respectively.

Patient A is a 17 years old and had her first seizure at age six. Her MRI was normal, but a PET scan revealed reduced metabolism of the left temporal and parietal lobes. Spontaneous seizures originated in the temporal lobe and spread posteriorly. A left temporal lobectomy was performed, leaving her seizure-free for the last two years (Engel class I [21]).

Patient B is a 12 year old with a history of developmental delay and seizures since 8 month of age. Before surgery she experienced as many as 30 seizures/day. Although her MRI was normal, a PET study revealed general hypometabolism of the cerebral cortex. She received a left frontal and occipital topectomy. She had an Engel Class III outcome.

Patient C is a 7 years old and the outcome was Engel class II 16 months after operation, while 3 years after surgery she has frequent seizures.

We have analyzed a total of 24 hours of ECoG recordings (mean 8 hours, range 200 minutes-15 hours 30 minutes), containing a total of 12 seizures (mean 4, range 3-5). The data were recorded with a sampling frequency of 400 Hz and band-pass filtered online to 0.5-50 Hz using moving overlapping windows and a finite impulse response filter with Kaiser window.

B. Synchronization Strength Diagrams

The information contained in the synchrograms can be easily employed to extract the level of phase synchronization between all the pairs of electrodes at our disposal. To this aim we define the strength of synchronization $S_{ij}(t)$ (SS) of every given electrode i to any other electrode j : we take the synchrogram of electrodes i and j , first divide the time axis into windows (in our case of 10 seconds), focusing on the line $(t_k) = 0$. In each such window, we calculate the number N_{ij} of phase points (shifted by π) within the range $[-0.01, 0.01]$. For $i \neq j$ $S_{ij}(t)$ is defined as N_{ij} normalized by the total number of phase points

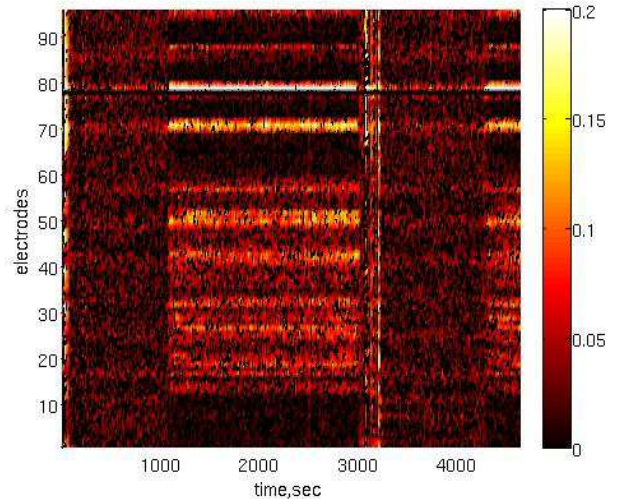


FIG. 6: (Color online) A typical SSD for a focal electrode [here, FG 14 ($i=78$)]. The electrodes here are numbered and the notation of the electrodes correspond to: 1-8 (AT1-AT8), 9-12 (ST1-ST4), 13-58 (PG13-PG58), 59-64 (PT3-PT8), 65-96 (FG1-FG32), cf. Fig 11 b. The time span of the diagram is 1 hour 30 minutes.

throughout the measured time interval, with t being assigned to the first time-point in the window. For $i=j$ we set $S_{ij} = 0$ for all times. Note that this procedure does not require time averaging and the choice of the time window is dictated by the signal. Precisely, if the time window is too large, short events of strong synchronization will be smeared out and not properly detected, thus reducing significantly the sensitivity of the method. On the other hand, a too short time window would result in a too small number of points over which the fraction is calculated, thus introducing strong noise in the evaluation of the synchronization strength. In the present case, we have chosen a window length of 10 seconds, that represents a good compromise to obtain maximum detail with minimal noise. The calculations were verified with time windows of 1 and 20 seconds.

The calculation is repeated for all signals as a reference in turn, since $S_{i,j} \neq S_{j,i}$ in general. The study of asymmetry is beyond the scope of this paper.

We refer to the diagram in which $S_{ij}(t)$ is displayed as the Strength of Synchronization Diagram (SSD). We color code the values of $S_{ij}(t)$ such that black is zero and white is the highest.

Two such typical diagrams [using as reference electrodes the specific electrodes FG 14 ($i=78$) and AT 5 ($i=5$)] and j from 1 to 96 are presented in Figs. 6 and 7. The electrodes in these figures are numbered in the montage order and correspond to: 1-8 (AT1-AT8), 9-12 (ST1-ST4), 13-58 (PG13-PG58), 59-64 (PT3-PT8), 65-96 (FG1-FG32). For the spatial relationship of these electrodes compare with Fig. 10 which shows the CT image and the two-dimensional projection of the actual place-

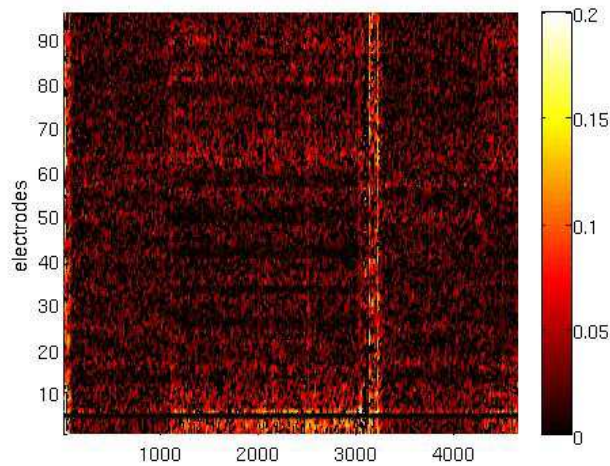


FIG .7: (Color online) A typical SSD for a non-focal electrode [here, AT 5 ($i=5$)].

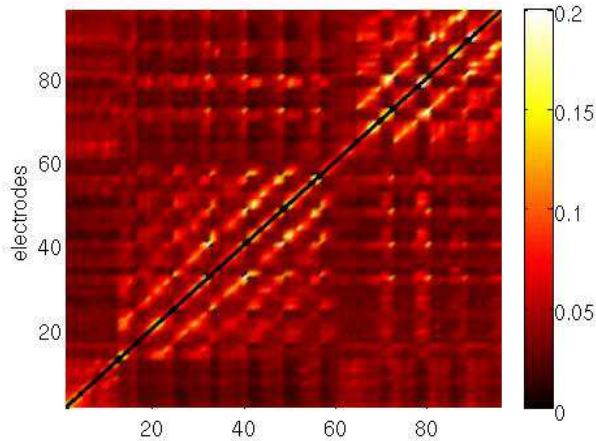


FIG .8: (Color online) A typical mean pair-wise synchronization matrix $S_{i,j,j}$, computed from the same S_{ij} as shown in Figs. 6 and 7, for the time interval (2000,2600) sec.

ment of the electrodes in this case (patient B). Note that a "strength of synchronization" of, say, 0.2, means that the signals are synchronized 20% of the time within the given time window.

The SSD provides a clear scenario of synchronization dynamics between two seizures. The diagram starts with the initial stages of the first seizure (ending at about $t=20$ seconds) with a high synchronization strength in almost all channels. Then the synchronization is lost for about 15 minutes. It then reappears at $t=1100$ seconds. In Fig. 6, showing SSD for the reference electrode FG 14, the most strong synchronization to the group of neighboring electrodes FG 6-8 ($i=70-72$), FG 15-16 ($i=79-80$) and FG 22-23 ($i=86-87$) is evident, while a larger group of electrodes is synchronized with FG 14 at

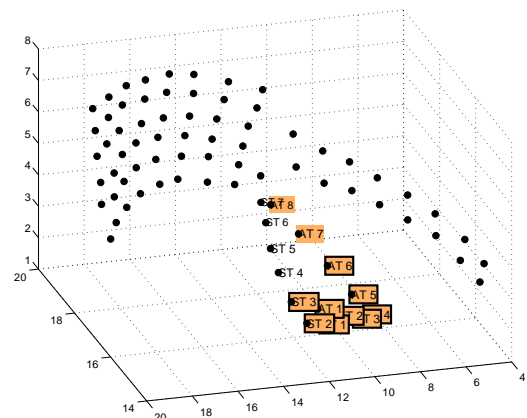


FIG .9: (Color online) The geometric spread of the electrodes, for the patient A. The viewing angle was chosen to best present the resected area. Only relevant electrodes are labeled. The electrodes with synchronization strength exceeding the threshold value S are marked by a rectangle. The electrodes chosen by the surgeons are highlighted.

lower strength. Interestingly, this electrode demonstrates similar level of synchronization strength with a spatially remote PG grid, especially with electrodes PG 49-PG 52 ($i=49-52$). At the same time, the electrode AT 5 (Fig. 7) becomes weakly synchronized with only few neighboring electrodes from the same strip. The next seizure occurs between $t=3000$ seconds and $t=3240$ seconds. Starting around $t=2940$ with a decrease in synchronization the event proceeds to exhibit high synchronization between all the electrodes, starting around $t=3000$. After $t=3240$ the synchronization is again lost and regained by FG 14 at about $t=4300$ seconds, as it did at $t=1100$.

It is crucial to stress that the SSD patterns presented in Figs. 6 and 7 are qualitatively preserved over all seizures of the same patient in our data. Moreover, the groups of strongly synchronized electrodes are preserved throughout all records, both when the patient B was awake and asleep, although at varying strength. The desynchronization following the seizure, apparent in Figs 6 and 7, corresponds to the post-ictal state, detected at the time of recording.

Similar behavior was found in the data of two other patients. In patient A's data only few pairs of electrodes remain synchronized during all available records, while only signals from the strips placed at the temporal lobe (AT and ST, cf. Fig. 9) were strongly synchronized during the seizure. For patient C three independent groups of strongly synchronized electrodes were found, while the overall behavior was similar to that of patient B.

Since the epileptic seizures imply high strengths of phase synchronization we identify the foci of epileptic activity with those regions that remain strongly synchronized at all times.

Thus our definition of the foci of epilepsy is the en-

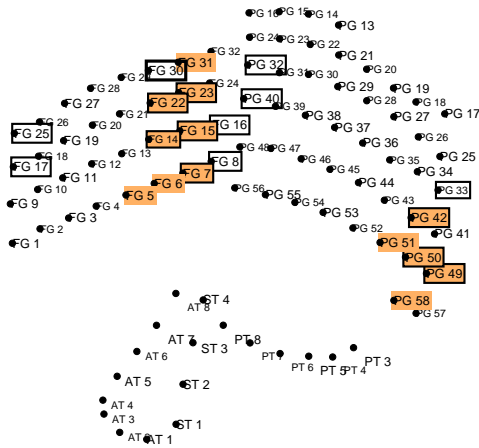
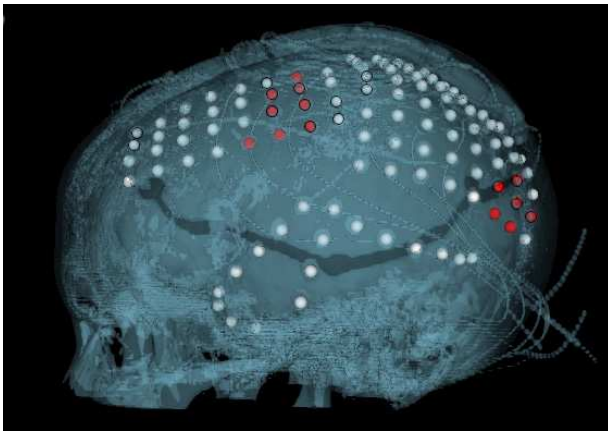


FIG. 10: (Color online) The CT image with marked electrodes (top) and the electrodes scheme (bottom), projected on the plane, for the patient B.

ensemble of those electrodes that, besides being strongly synchronized to each other during the ictal period, remain also synchronized above a chosen threshold during the inter-ictal period. To identify this ensemble we now compute the time average of S_{ij} according to

$$S_{ij} = \frac{1}{T} \sum_{t_k=1}^T X_i^T X_j^T ; \quad (3)$$

where the time interval $(1; T)$ does not include a seizure. An example of the resulting mean pair-wise synchronization matrix S_{ij} is shown in Fig. 8. S_{ij} converges well for $T > 60$ seconds. The synchronization strength within the given grid is higher than between spatially remote grids. Defining the mean S as

$$S = \frac{1}{N_i N_j} \sum_i \sum_j X_i^T X_j^T ; \quad (4)$$

for the S_{ij} shown in Fig. 8, S within the grid is 0.056 (range 0.047 - 0.065) within standard deviation

= 0.01 (range 0.0058 - 0.013), while the inter-grid S is 0.038 (range 0.031 - 0.04) within $S = 0.004$ (range 0.002 - 0.006). At the same time, the SS of the strongly synchronized group ranges in the interval 0.1 - 0.2, being more than three standard deviations above the corresponding mean value. The difference is especially striking for the inter-grid synchronization, found between the group in FG grid (FG 6-7, FG 14-16), and the remote group in PG grid (PG 49, PG 50). Similar values of S_{ij} were found for patients A and C, although no such remote synchronization was detected.

To localize the foci we need to choose a threshold value S_{th} , such that only electrode pairs with $S_{ij} > S_{th}$ will be selected as belonging to the focus. Clearly, the number of selected electrodes is a strong function of S_{th} . To compare with the actual surgeons selection we chose S_{th} , such that the number of electrodes designated by the present procedure agrees as much as possible with the number chosen by the surgeons. It turned out that chosen values of S_{th} are larger than the value of S by at least three standard deviations.

The results, that refer to calculations over the entire set of available data, are displayed in Fig. 9-11. We color those electrodes that were chosen by the surgeons for the operation, and we put a rectangle on every electrode that is identified by our method.

For patient A the SS was relatively low in the inter-ictal periods with only two pairs of electrodes strongly synchronized. On the other hand, during the seizure, the entire region, covered by AT and ST strips was synchronized at a level of 0.6-0.7. We included in the selection 9 electrodes, that showed highest mutual synchronization. They all are placed within the resected area. This patient was seizure-free after the surgery.

We have shown in Figs 6-8 that patient B had two remote groups of electrodes that remained inter-ictally synchronized. As seen in Fig 10, the chosen subset of strongly synchronized electrodes overlap with both foci, resected during surgery. Out of 12 electrodes marked by surgeons, 8 were identified also by us. However, we have found also other electrodes, that belong to the same focus (in the grid FG), as well as adjacent electrodes from the grid PG. The outcome of the surgery was an improvement in patient's condition, who however did not become seizure-free.

As for patient C, the operated area and our chosen set of electrodes overlap only partially. Out of 30 electrodes marked by surgeons, only 9 were chosen also by us. An additional strongly synchronized group was found at the edge of the PG grid, indicating the possibility for another, not resected focus. After initial improvement, this patient did not benefit from the surgery.

In summary, we pointed out that a simple and computationally fast method to detect phase synchrony in ECoG signals is able to detect and localize the multiple foci of epilepsy. The method does not require any assumptions about the spectral features of the signal or the nature of the synchronization between the signals.

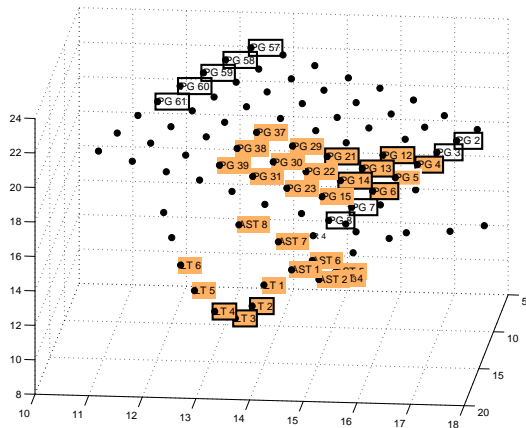


FIG. 11: (Color online) The electrodes scheme for the patient C. The viewing angle was chosen for best presentation of the resected areas. Only relevant electrodes are labeled for clarity. The electrodes are marked as in Fig. 9.

The measurement of the synchronization strength from the synchrogram amounts to a straightforward count of the data points within a chosen interval. The synchronization dynamics in the long recordings reveal repeated

patterns, allowing to distinguish different stages of evolution from one seizure to another. For each patient, we found a subset of electrodes, that remained strongly synchronized at all times, regardless of the physiological conditions, such as sleep. These subsets overlap fully or partially with the areas chosen for resection. In patient B we correctly identified the existence of two distant foci. In patient C we also identified the presence of additional focus, not operated on. The overlap of the location of the electrodes identified by our method and the resected areas is consistent with the degree of surgery success.

While it is not reasonable to draw any general conclusions on the basis of the study of only three patients, our observations nevertheless indicate that the method can be a practical tool for surgeons to optimize the surgery outcome with minimizing the risk of post-operative morbidity.

Acknowledgments

We thank Itai Doron and Tomer Gazit for fruitful discussions. This work was partially supported by a EU grant under the GABA project. S.B. acknowledges a visiting fellowship granted by the Yeshaya Horowitz Association through the Center for Complexity Science.

-
- [1] Surgery for Epilepsy. NIH Consensus Statement Online 1990 Mar 19–21 [1990 Mar 19–21];8(2):1–20.
- [2] S.J. Schi, Nature Medicine 4, 1117 (1998); B. Litt and J. Echauz, The Lancet Neurology 1, 22 (2002); I. Doron, E. Hulata, I. Baruchi, V.L. Towle and .Ben Jacob Phys. Rev. Lett. 96 258101 (2006).
- [3] J.Ph. Lachaux, D. Rudrauf and P. Kahane, J. Physiol. (Paris) 97, 613 (2003).
- [4] Widman et al., Epilepsia 41, 811, 2000;
- [5] Lehnertz et al., J. Clin. Neurophysiol. 18, 209, 2001
- [6] P. Grassberger and I. Procaccia, Physica D 9 189, (1983), Phys. Rev. Lett. 50 346, (1983).
- [7] J. Amhold, P. Grassberger, K. Lehnertz, C.E. Elger, Physica D 134 419 (1999).
- [8] Le Van Quyen et al., Brain Res. 792, 24, 1998; M. Le Van Quyen, J. Martinerie, C. Adam, F.J. Varela, Physica D 127 250, (1999).
- [9] Andrzejak et al., Epilepsy Res., 69, 30, 2006
- [10] F. Takens, in: D.A. Rand, L.S. Young (Eds.), Lecture Notes in Mathematics, vol. 898, Springer, Berlin, 1981, p. 366.
- [11] I. Procaccia, Nature 333, 498 (1988).
- [12] C.J. Stam, B.W. van Dijk, Physica D 163, 236 (2002).
- [13] R. Quian Quiroga, T. Kreuz and P. Grassberger, Phys. Rev. E 66, 041904 (2002).
- [14] K. Schindler, H. Leung, Ch.E. Elger and K. Lehnertz, Brain 130, 65 (2007).
- [15] S. Bialonski and K. Lehnertz, Phys Rev E 74, 051909, 2006;
- [16] C.A. Schevon et al., NeuroImage 35, 140 (2007)
- [17] M. Palus et al., Phys Rev E 63, 046211, 2001
- [18] M.G. Rosenblum, A.S. Pavlovsky and J. Kurths, Phys. Rev. Lett. 76, 1804 (1996); S. Boccaletti, J. Kurths, D.L. Valladares, G. Osipov and C.S. Zhou, Phys. Rep. 366, 1 (2002).
- [19] P.E. McSharry, L.A. Smith and L. Tarassenko, Nature Medicine 9, 241 (2003).
- [20] S. Schäfer, M.G. Rosenblum, J. Kurths and H.H. Abel, Nature 392, 239 (1998).
- [21] Engel J Jr, van Ness PC, Rasmussen TB, Ojemann LM (1993). Outcome with respect to epileptic seizures. In: J. Engel, Jr. (ed.), Surgical Treatment of the Epilepsies, 2nd ed. New York: Raven Press, pp. 609–621.
- [22] S. Boccaletti, V. Latora, Y. Moreno, M. Chavez and D.-U. Hwang, Phys. Rep. 424, 175 (2006).